Applied Surface Science 257 (2010) 1247–1253

Contents lists available at ScienceDirect

Applied Surface Science

journal homepage: www.elsevier.com/locate/apsusc

Plasma-mediated ablation of biofilm contamination

Zhixiong Guo*, Xiaoliang Wang, Huan Huang

Department of Mechanical and Aerospace Engineering, Rutgers, The State University of New Jersey, 98 Brett Road, Piscataway, NJ 08854, USA

ARTICLE INFO

Article history:
Received 5 May 2010
Received in revised form 23 July 2010
Accepted 9 August 2010
Available online 13 August 2010

Keywords:
Surface decontamination
Ultra-short pulsed lasers
Plasma-mediated ablation
Biofilms
Blood contamination

ABSTRACT

Ultra-short pulsed laser removal of thin biofilm contamination on different substrates has been conducted via the use of plasma-mediated ablation. The biofilms were formed using sheep whole blood. The ablation was generated using a 1.2 ps ultra-short pulsed laser with wavelength centered at 1552 nm. The blood contamination was transformed into plasma and collected with a vacuum system. The single line ablation features have been measured. The ablation thresholds of blood contamination and bare substrates were determined. It is found that the ablation threshold of the blood contamination is lower than those of the beneath substrates including the glass slide, PDMS, and human dermal tissues. The ablation effects of different laser parameters (pulse overlap rate and pulse energy) were studied and ablation efficiency was measured. Proper ablation parameters were found to efficiently remove contamination with maximum efficiency and without damage to the substrate surface for the current laser system. Complete removal of blood contaminant from the glass substrate surface and freeze-dried dermis tissue surface was demonstrated by the USP laser ablation with repeated area scanning. No obvious thermal damage was found in the decontaminated glass and tissue samples.

1. Introduction

Surface cleaning is a very broad field that concerns destroying and/or removal of contaminants like chemical agents, medical/biological wastes, radioactive wastes, metal oxides, bacteria, or microorganisms, etc., from the surface of a material. It is important in many biomedical and industrial processes and applications. Quite a few decontamination techniques have long been developed, practiced and matured over time. For example, cleaning and disinfection in the food industry [1] are traditionally performed with chemical agents diluted in water or with steam vacuuming and hot water washing. However, such traditional surface cleaning techniques usually produce large quantity of liquid which are polluting or environmentally unfriendly, especially when the removed contamination is hazardous, which poses challenge to its disposal.

Many non-disposable devices, surgical instruments and dental implants are used in the hospital and clinical environment. Historically, sterilization was done mainly through physical methods, especially using moist heat in the form of steam autoclaves as well as dry heat. Nowadays, however, hospitals possess a greater number and diverse types of expensive, intricate instruments [2]. Therefore, alternative technologies [3] were developed while high heat wet or dry is not a good option for all instruments. These include chlorine dioxide gas, ozone gas, gas plasma sterilization, and ionizing radiation, etc.

Furthermore, removal of unwanted materials, especially contaminants, from the surface of allograft, xenograft, and autograft tissues is important for preparing the tissue for implantation [4]. However, there are few methods that can effectively remove unwanted material without harming or damaging the tissue. Common methods like applying solutions comprising peracetic acid, povidone–iodine, or mixtures of antibiotics can vary in efficacy. Moreover, gamma irradiation can alter the structural and biomechanical properties of the tissue. For instance, irradiation of patellar tendon grafts may reduce the mechanical strength of the tendon, while irradiation of skin grafts may induce cross-linking of the skin matrix and cause the graft to stiffen [4]. Therefore, it would be useful to develop an effective method of removing unwanted materials and contaminants from the surface of graft tissues without damaging or altering the properties of the tissue.

Microorganisms present upon the surfaces of apparatus and tissues easily form a thin biofilm. Adhesion forces make biofilms difficult to eliminate by detergents and mechanical action [5]. Bacteria in biofilms are more resistant to treatment with disinfectants than bacteria suspended in liquid media. Recently, Sadoudi et al. [6] assessed the efficacy of nanosecond (ns) pulsed laser beams (1064, 532 and 355 nm, and 20 ns pulses) for removal and killing of adherent bacteria from stainless steel surfaces. It is well-known that laser technology holds several advantages that make it superior in surface decontamination: non-intrusive, precise, dry or wet.

Surface cleaning and modification with pulsed lasers have attracted much attention in the past decade. For example, Theppakuttai and Chen [7] produced nanopatterns on borosilicate glass using a Nd:YAG laser (1064 nm, 10 ns). Effects of laser intensity and

* Corresponding author. Tel.: +1 732 445 2024; fax: +1 732 445 3124.
E-mail address: guo@jove.rutgers.edu (Z. Guo).

0169-4332/$ – see front matter © 2010 Elsevier B.V. All rights reserved.
doi:10.1016/j.apsusc.2010.08.033

repetition rate on ablative cleaning of copper oxides were investigated both numerically and experimentally by Zhang et al. [8] using a frequency-tripled Nd:YAG laser (355 nm, 50 ns pulses). Tam et al. [9] invented the steam laser cleaning technique in which excimer laser pulses typically in 1–100 ns were utilized to remove small particulates in hi-tech manufacturing. She et al. [10] extended the steam laser cleaning to near-infrared laser irradiation. Bereznai et al. [11] modified titanium implant surfaces with ns and sub-ps excimer laser pulses. Excimer laser ablation was also applied to the removal of radioactive contamination [12,13]. In these studies, the removal of material is based on laser ablation with low radiation intensity in which the material is heated by the absorbed laser energy and evaporates or sublimates [14]. The ablation effect depends on the material's optical properties and the laser wavelength.

Nowadays surface processing with ultra-short pulsed (USP) lasers that have a pulse duration from picoseconds (ps) down to femtoseconds (fs) has emerged as a promising method because of its prominent advantages in a wide range of materials, including semiconductors [15], glasses [16,17], metals [18] and polymers [19]. USP laser ablation is governed by plasma-mediated ablation, also known as optical breakdown, in which ablation is primarily caused by plasma ionization and does not depend on the surface properties or material characteristics. This means that even the most intractable materials, such as refractory metals or transparent materials, can be cleanly and congruently ablated [20]. A key benefit of USP laser pulses over nanosecond or other longer pulsed lasers, lies in its ability to deposit high energy into a compact material volume in an extremely short time period before thermal diffusion ever takes place, leading to precise micromachining and processing with minimized thermal and collateral damage. USP lasers have also been applied to the biomedical field. Examples include killing of embedded cancerous tissue [21], tissue welding and soldering [22], bio-imaging [23], and removal of adhesive cells [24], to name a few. To the authors' knowledge, however, removal of biofilm contamination using a USP laser has not been reported in the literature.

In this work we apply USP laser pulses to remove blood biofilm contamination on glass, PDMS and tissue substrates surfaces. Whole sheep blood was used to form an adhering biofilm on a glass substrate or tissue surface. First, the single line ablation features were studied and the laser ablation threshold for blood film and bare substrates was investigated. Then the effects of different laser parameters were examined. Finally, complete removal of a layer of blood biofilm contaminant from a glass substrate surface and a real human tissue surface was carried out and demonstrated.

2. Materials and methods

2.1. Laser

The surface decontamination experiments were performed using an erbium doped fiber laser (Raydiance, Inc.) operating at wavelength 1552 nm with pulse duration of 1.2 ps. The laser beam parameters such as pulse energy and repetition rate are controlled by a control system. Its pulse repetition rate is tunable between 1 Hz and 500 kHz. The direct output energy of the laser is adjustable between 1 and 5 μJ per pulse.

2.2. Substrate materials

Three exemplary substrate materials were used in the experiments, i.e., glass, poly(dimethylsiloxane) (PDMS) and human skin tissue. The glass used in this experiment is typical microscopic glass slides. PDMS is one of the most widely used silicon-based polymers. It is optically clear, inert, non-toxic and non-flammable. PDMS samples were prepared by Dow Corning sylgard elastomer 184 kit. Proper amounts of PDMS base and curing agent were taken by weighing scale 10:1 and mixed well to a milky color consistency. The mixture was put into a vacuum chamber to evacuate the bubbles generated during mixing. The degassed PDMS assembly was placed on a hotplate at 65 °C for 4 h upon completion of the curing cycle. The PDMS samples prepared were about 3 mm thick.

For the tissue substrate, freeze-dried dermal tissues were used in this study. Human dermis samples packaged in hydrated state were prepared and provided by Musculoskeletal Transplant Foundation (MTF). The wet soft tissue was precut into proper portions and put into a freezer (−20 °C). The tissue will become completely dry over a period of 12 h and the samples can be stored at room temperature over a long period—months to years.

2.3. Contaminant

Blood is a very common type of contamination present to medical or surgical device surface. In the experiments sheep whole blood with anticoagulant citrate (Hemostat Laboratories) was used to form biofilms as surface contaminants on different substrates. The blood was preserved in a refrigerator at 4 °C. Before experiment the blood was smeared onto the surface of the substrates as contamination and exposed in air at room temperature for 12 h until it was completely dry. Then a thin biofilm of bloodstain was formed on the substrate surface. The thickness of the blood biofilm was measured between 3 and 10 μm typically.

2.4. Experimental setup

Fig. 1 shows the sketch of the experimental setup. The output beam is modified by an astigmatism correction mirror and a routing mirror before launched into a long working distance objective lens (Mitutoyo M Plan Apo NIR 20×, NA = 0.40). The focal length (f_L) of the lens is 20 mm and the incident beam on the lens has a diameter about 10 mm. The diffraction-limit focal spot diameter ($1/e^2$) of the focused laser beam in free space is estimated at 8 μm. The beam energy loss through the optical system is about 49%.

The sample is fixed to a lab-made altitude-adjustable stage which is stabilized on a 3D automated precision compact linear stage (VP-25XA, Newport). This 3D stage is controlled by the laptop control system. The working distance is justified through the observation of the ablation spark. To achieve line or area ablation, the sample moves with the stage in the x–y plane so the focused spot is rastered across the ablation surface. To collect the aerosols formed from the removed matter, an extraction vacuum (FX225, EDSYN) is used and the extraction nozzle is pointed at the sample surface with about 3 cm clearance.

2.5. Measurement

After laser processing, the samples were checked and characterized with an upright digital microscope (National Optical DC3-156-S) and a scanning electron microscopy (SEM, AMRAY 1030I). The depths of ablation and blood films are measured by a stylus profiler (Dektak 3030).

3. Results and discussion

Plasma-mediated ablation occurs when the incident pulse flux exceeds the threshold for optical breakdown [25]. The reported threshold value varied in a wide range. For instance, Niemz [25] specified a general value 10^{11} W/cm^2 for solids. Ben-Yakar and Byer [26] determined a single shot ablation threshold fluence 2.6 J/cm^2 ($\sim 10^{13}$ W/cm^2) and a multishot threshold 1.7 J/cm^2 for laser ablation of borosilicate glass using pulses of 200 fs duration, centered

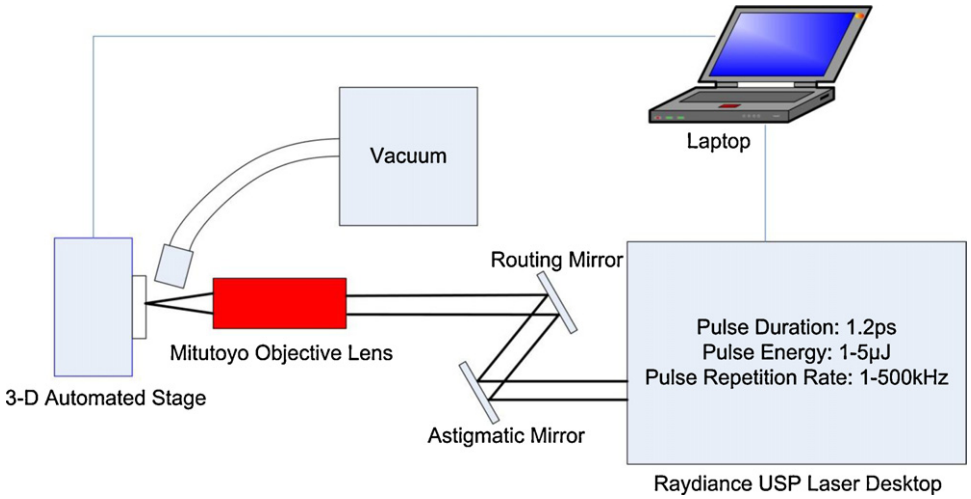

Fig. 1. Schematic diagram of the experimental setup.

at 780 nm wavelength. Loesel et al. [27] measured the threshold fluence for neural tissue to be about 5.3 J/cm^2 ($\sim 10^{12}$ W/cm^2) for 3 ps laser pulses at 630 nm; and 1.5 J/cm^2 for 100 fs pulses from the same laser.

For decontamination of a biofilm, overlap of ablation spots is necessary in order to achieve continuous and complete ablation in a finite area. To this end, ablation features of surface line scanning and the ablation threshold must be understood. The single line ablation experiments were first carried out to investigate the effects of pulse energy and pulse overlap rate on the line ablation. The irradiation pulse energy, that is 51% of the laser output energy, determines whether the incident laser fluence exceeds the ablation threshold. The pulse overlap rate is the ratio of the pulse repetition rate, over the moving speed of the work stage.

Fig. 2 shows the microscope view (400×) of four single line ablations at a blood film on a glass slide with different pulse energies. The experiments were carried out at a constant pulse repetition rate of 20 kHz and a constant stage moving speed of 20 mm/s; and thus, the pulse overlap rate is constant at 1 pulse/μm. Lines 1–4 in Fig. 2 correspond to irradiation pulse energy 2.55, 2.04, 1.53 and 1.02 μJ, respectively.

Fig. 3(a) and (b) shows the microscope views (400×) of four single line ablations at bare glass substrate and PDMS, respectively. The pulse overlap rate is 1 pulse/μm. Four different irradiation pulse energies from 2.28, 2.02, 1.54, to 1.04 μJ are considered.

For laser pulses with a Gaussian spatial beam profile, the ablation feature size can be expressed as [28]:

$$D^2 = 2r_{\text{eff}}^2 \ln\left(\frac{F_0}{F_{\text{th}}}\right), \quad (1)$$

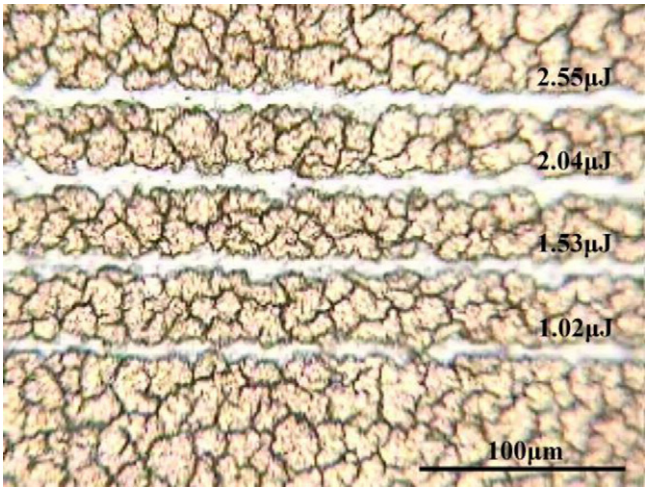

Fig. 2. Microscopic picture (400×) of single line ablations at blood film with 1 pulse/μm and different pulse irradiation energies: 2.55, 2.04, 1.53 and 1.02 μJ for lines 1–4, respectively.

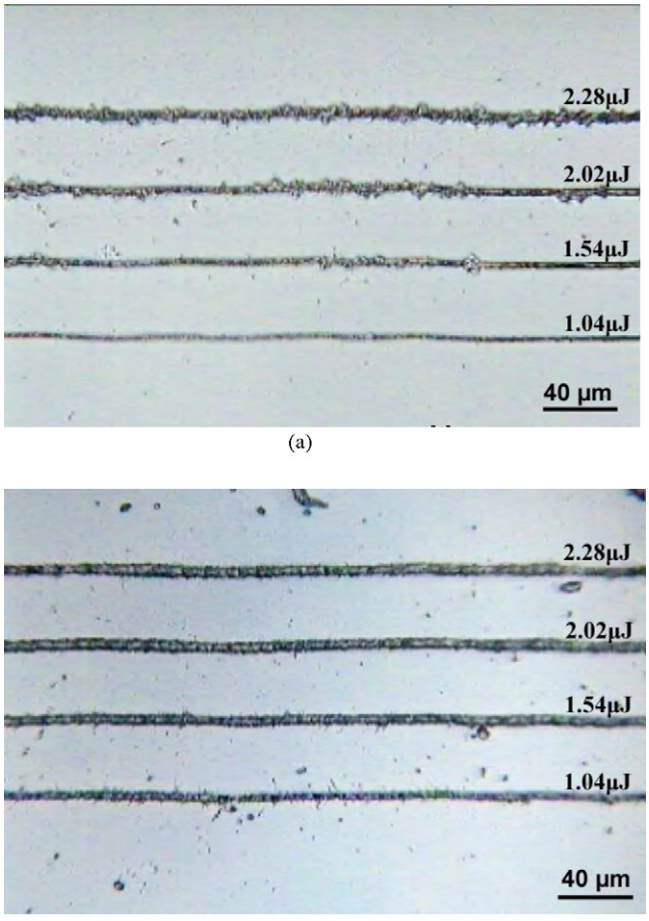

Fig. 3. Microscopic pictures (400×) of single line ablations with 1 pulse/μm and different pulse irradiation energies 2.28, 2.02, 1.54 and 1.04 μJ from top to bottom: (a) bare glass substrate and (b) bare PDMS substrate.

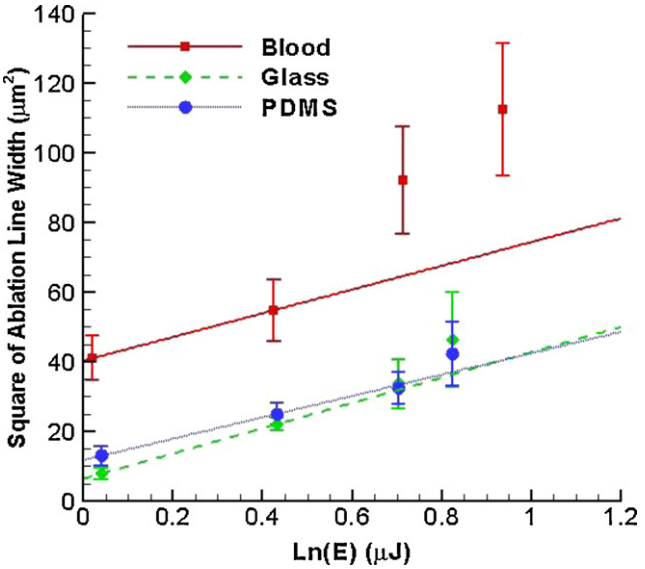

Fig. 4. Square of ablation line width versus pulse irradiation energy for ablation at different materials.

where D is the diameter of the ablation crater, F_0 is the maximum laser fluence on the sample surface, F_{th} is the ablation threshold fluence, and r_{eff} is the effective radius of the focal spot. The maximum irradiation fluence can be calculated from the irradiation pulse energy E as

$$F_0 = \frac{2E}{\pi r_{eff}^2}. \quad (2)$$

Therefore, it is possible to determine the effective radius and the ablation threshold by plotting the square of the diameter of the ablation crater versus the irradiation pulse energy. An ablation line consists of continuously ablated craters along the laser scanning direction. When the pulse overlap rate is so intense that no individual craters can be distinguished, the ablation line width is then equivalent to the diameter of the ablated crater generated by many repeated pulses [29,30].

Fig. 4 shows the linear fittings of the square of the measured ablation line width versus the logarithm of the pulse irradiation energy for the three different materials shown in Figs. 2 and 3, i.e., blood film, glass, and PDMS. The effective radii for the focal spots with different materials can be calculated by the slopes in Fig. 4 and after obtaining the effective focal radius, the fluence can be calculated by Eq. (2) and the thresholds for different pulse overlap rates can be acquired by extending the fitted lines in Fig. 4 to intersect with the abscissa.

Table 1 lists the effective focal spot radii and ablation thresholds determined by the present study for blood film, glass, and PDMS with 1 pulse/μm pulse overlap rate. The measured threshold of the microscopic glass slide (2.88 J/cm^2) is very close to the reported threshold value (2.6 J/cm^2) of borosilicate glass [26]. As shown in Table 1, the effective focal spot radius is very close to the diffraction-limit spot size, and the ablation threshold of the blood contaminant is smaller than those of the bare substrates and the different thresholds for the blood contaminant and bare substrates permits selective ablation of the contaminant from the substrates. And from a previous study [31], the threshold for freeze-dried dermis (3.20 J/cm^2 for 1 pulse/μm) is also greater than that for the blood contamination. As pointed out by Zoppel et al. [32] and Meyer et al. [33], the range of fluences between the thresholds of contaminant and substrate defines a process window where the contaminant can be selectively removed from the substrates.

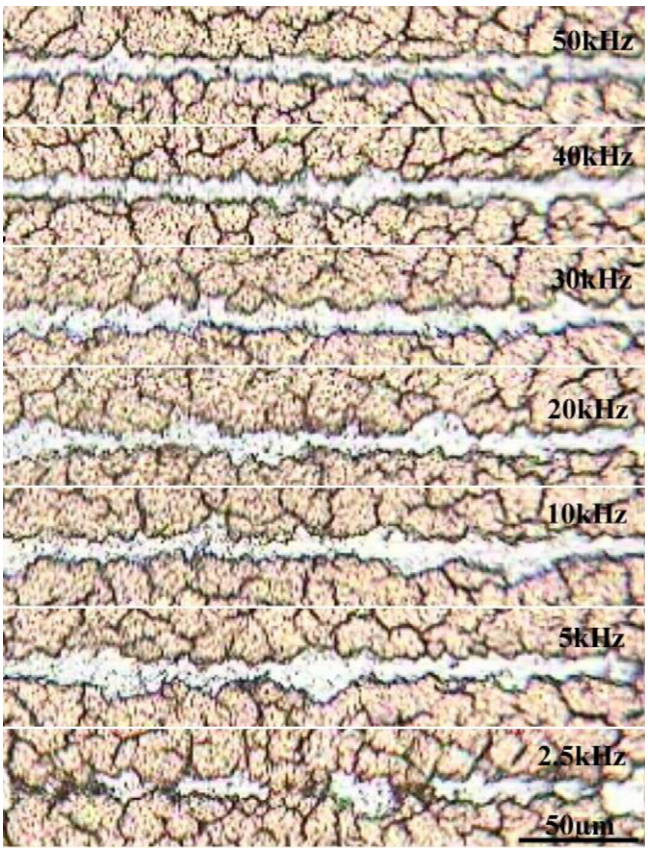

Fig. 5. Microscopic pictures (400×) of single line ablations at blood film with different pulse overlap rates.

Single line ablation of blood biofilm and bare substrates with different pulse overlap rates was carried out to study the effect of the pulse number. Fig. 5 shows the single line surface ablation of blood biofilm on glass slide with different pulse overlap rates. The stage moving speed is fixed at 20 mm/s so that the pulse overlap rate is linearly proportional to the pulse repetition rate. The repetition rate varies from 2.5 kHz through 50 kHz, which rends a pulse overlap rate from 0.125 to 2.5 pulses/μm. The irradiation pulse energy is set to be 2.55 μJ. For the case at 2.5 kHz in as shown in a picture in Fig. 5 (corresponding to 0.125 pulses/μm), discontinuous ablation is observed and the blood contaminant cannot be completely removed for the scanned line area. For the cases with pulse overlap rates above 0.5 pulse/μm, the ablation continuity is pretty good and the overlap of the ablation spot can fully remove the contaminant. An appropriate pulse overlap rate is crucial to achieve satisfying ablation effect with high ablation efficiency as well as complete contaminant removal without thermal damage. In the previous studies, 1–2 pulses/μm pulse overlap rate for 1.0–2.0 μJ pulse energy was found for PDMS internal layer separation [32]

Table 1
Ablation thresholds for different materials at pulse overlap rate 1 pulse/μm.

Material	Blood contaminant	Glass substrate	PDMS substrate
Effective focal spot radius (μm)	4.1	4.3	4.2
Threshold F_{th} (J/cm^2)	1.16	2.88	2.65

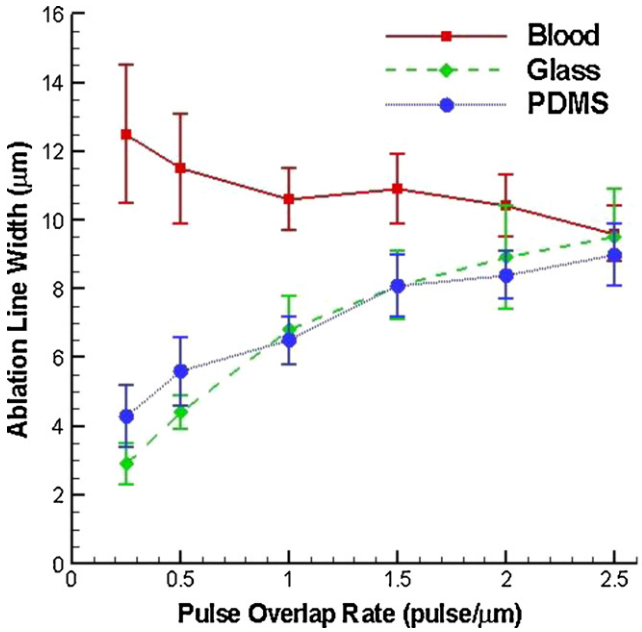

Fig. 6. Ablation line width versus pulse overlap rate for ablation at different materials.

and 5 pulses/μm and 1.5 μJ were used for wet dermis tissue separation [33]. In this study, 1 pulse/μm was found as an appropriate pulse overlap rate for decontamination of blood biofilm.

Fig. 6 shows the measured single line surface ablation line widths with different pulse overlap rates for the blood biofilm, bare glass and PDMS, respectively. For the bare glass and PDMS, the line widths exhibit an increasing trend with the increase of the pulse overlap rate; but when the overlap of the pulse reaches a certain level, for example 1 pulse/μm, the line widths grow very slowly as the pulse overlap rate increases. Contrary to our expectation, the line width on blood stain surface exhibits a small decreasing tendency initially with the increase of pulse overlap rate, after that it flattens. The ablation feature is a combination of the complex effects of plasma-mediated ablation, the acoustic wave generated by the laser pulse, and ejection of particles and expansion of plasma and vapor.

As shown in Fig. 6, the widths of the single line ablation on the blood contamination layer exhibit relatively large fluctuation as compared with the line scanning results on rigid dielectric materials like the glass and PDMS polymer. This is due to the difference in the properties of the materials. The dry blood biofilm is not a rigid isotropic material. For these three materials, the dominating ablation effect is the plasma-mediated ablation, and when the pulsed laser energy is delivered to the surface and absorbed, material within the focal volume is transformed into plasma and ejected away from the surface. But when this happens in the focal volume for the case of the blood biofilm, the expansion and ejection of the plasma vapor plume also blow non-negligible amount of surrounding material away from the surface, due to the floppy nature of the dry bloodstain. The amount of material taken away depends on the different local material morphology, such as the crack formed during the drying process and direction of the crack, resulting in large fluctuation of the scanning line width. The uniformity of line scanning feature (low deviation of scanning line width) is very crucial in precise micromachining. For applications to surface decontamination in a large area, however, uniformity in a single line may be not strictly required because the overlap of many scanning lines can be controlled to make sure the processed area reach required cleaning effect.

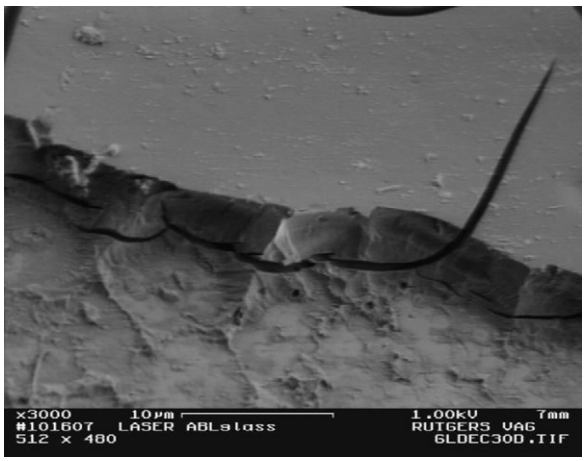

Fig. 7. SEM image of an ablation edge of blood film on a glass slide (2.55 μJ, 1 pulse/μm).

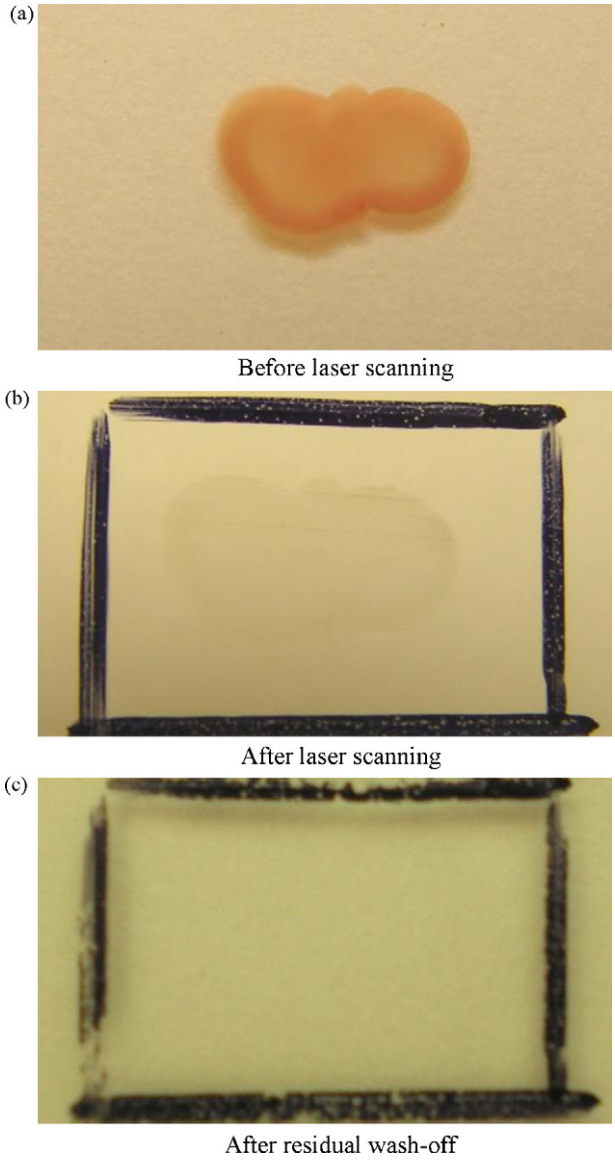

Fig. 8. Demonstration of blood decontamination on a glass substrate: (a) before laser scanning; (b) after laser scanning; and (c) after residual wash-off.

Fig. 7 shows an SEM image of one edge of the laser ablation of blood contaminant (2.55 μJ and 1 pulse/μm). The edge of the scanned area is shown in order to compare the ablated and non-ablated surfaces. The crack in the contamination blood layer was formed from the drying process of the blood film before the laser ablation experiment. Similar cracks can be observed all over the contamination area under a microscope (refer to Figs. 2 and 5). From the SEM picture we can see that there is still small amount of residue attached to the surface while the bulk blood contamination is removed. From the measurement by a stylus profiler, the ablation depth for 2.55 μJ irradiation pulse energy reached the total thickness of the contamination layer, which is about 3.5 μm on average. Further parametric studies could give us a window of appropriate laser parameters that would remove the contamination layer with no damage or limited damage to the substrate at a given thickness.

Furthermore, an area scanning was carried out to achieve area decontamination effect. Multiple successive scanning lines were densely arrayed and overlapped and an evenly area scan was formed. The scanning lines are spaced 2 μm between two consecutive scanning lines and the line spacing between two consecutive lines is also 2 μm in order to realize a good area ablation effect despite of the ablation inconsistency caused by the factors such as vibration and wavy motion of the stage, surface morphology variation. Fig. 8 demonstrates blood biofilm decontamination in a large area on glass substrate which was carried out with 2.55 μJ irradiation pulse energy and 1 pulse/μm pulse overlap rate. Comparing Fig. 8(a) (view before USP laser scanning) with Fig. 8(b) (view after the USP laser area scanning), we can clearly observe the removal of the contamination. The dimension of the marked black frame in Fig. 8(b) and (c) is about 11 mm long and 8 mm wide. In this experiment the focal spot was carefully aligned right above the surface so that a good decontamination effect can be achieved. As shown in Fig. 8(b), after one time area scanning most of the blood contamination was removed. Fig. 8(c) shows the view of the glass slide after washing away the residual existed in Fig. 8(b). No visible damage can be seen on the substrate glass surface and the surrounding area as shown in Fig. 8(c). The surface was very flat and no any melting or charring mark was found under microscopic view. A micrometer measured no thickness change in the glass slide.

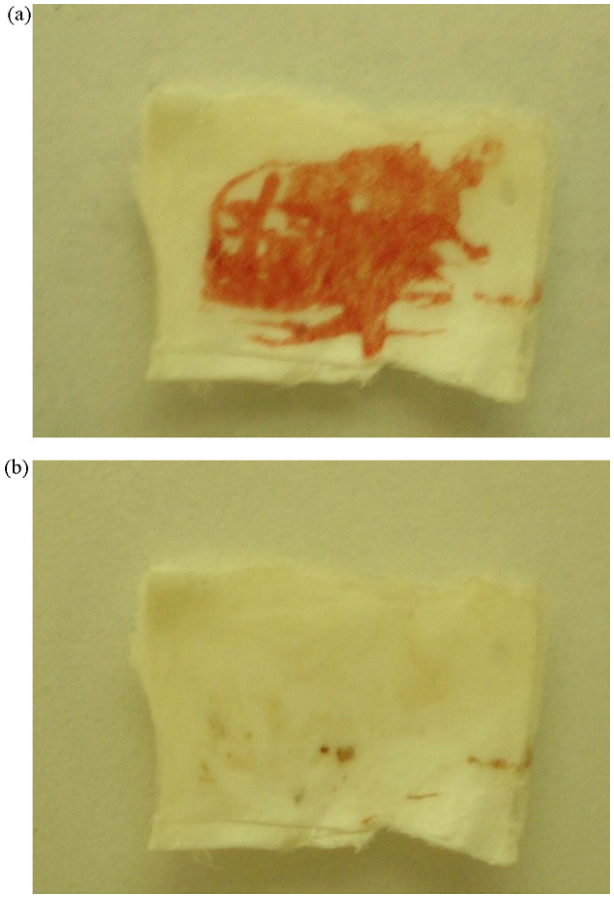

Fig. 9. Blood decontamination on a freeze-dried dermis tissue: (a) before surface decontamination and (b) after USP laser surface decontamination.

Fig. 9 demonstrates the decontamination of blood biofilm on another substrate—freeze-dried dermis tissue surface, which is one of the commonly used materials for tissue grafting and implantation. Fig. 9(a) shows the freeze-dried dermis with a layer of blood contaminant in a large area of the dermal tissue surface. The total dimension of the tissue sample is about 11 mm long and 6 mm wide. Four times repeated area scan were carried out with 2.55 μJ irradiation pulse energy and 1 pulse/μm pulse overlap rate with 2 μm spacing between two consecutive scanning lines. Since the flatness of a freeze-dried dermis sample is not as good as a glass substrate, after each area scan the beam focal plane was adjusted towards the sample for 50 μm and totally three times adjustments were needed to ensure that the contaminant was fully removed. As shown in Fig. 9(b), the blood contaminant was nearly removed completely and only some minor spots of blood were left because of the existence of the irregular small dents and holes on the tissue surface. No obvious thermal damage was found after the decontamination experiment.

4. Conclusion

Ultra-short pulsed infrared laser ablation features and thresholds were studied on blood contamination with comparison to transparent dielectric materials like glass and PDMS polymer. The single line ablation features have been measured and the ablation thresholds of the blood contamination and the bare substrates were determined. The thresholds under the specified condition are found to be 1.16, 2.88, and 2.65 J/cm^2 for the blood film, bare glass, and PDMS, respectively. Since the threshold for the blood contamination is lower than those for the beneath substrates including glass, PDMS, and human dermal tissue, it is ideal to consider this USP laser selective blood decontamination technique on the surfaces of these substrates. The ablation effects with different pulse overlap rates were investigated and the ablation efficiency was measured. An appropriate overlap rate of 1 pulse/μm is found for the blood decontamination.

The applications of the USP laser ablation to surface decontamination in medical industrial scale were demonstrated in a large area of glass and freeze-dried dermis tissue substrates. No obvious damage was found to the beneath substrates after the removal of the blood thin film. Therefore, with appropriate laser parameters and precise alignment control the contamination can be perfectly removed without causing any damage to the substrates. Given the advantage of limited damage effect by the USP laser ablation, the potential of this technique to applications including decontamination and material removal on soft biological tissue surface is high.

Acknowledgements

Support of this work by the Musculoskeletal Transplant Foundation, Raydiance, Inc., and the Charles and Johanna Busch Memorial Fund managed at Rutgers University, is gratefully acknowledged. Part of this material is also based on the work supported by the National Science Foundation under Grant No CBET-0827473.

References

[1] H. Dincer, T. Baysal, Crit. Rev. Microbiol. 30 (3) (2004) 197–204.
[2] R.A. Slaybaugh, Infection Control Today (2000) June issue, see also www.infectioncontroltoday.com/articles/061feat3.html.
[3] M. Moisan, J. Barbeau, M.C. Crevier, J. Pelletier, N. Philip, B. Saoudi, Pure Appl. Chem. 74 (3) (2002) 349–358.
[4] A. Gertzman, M. Schuler, Private Communications, the Musculoskeletal Transplant Foundation, 2007.
[5] L. Boulange-Petermann, B. Baroux, M.N. Bellon-Fontaine, J. Adhes. Sci. Technol. 7 (3) (1993) 221–230.
[6] K. Sadoudi, J.M. Harry, O. Cerf, Lett. Appl. Microbiol. 24 (3) (1997) 177–179.
[7] S. Theppakuttai, S.C. Chen, Appl. Phys. Lett. 83 (4) (2003) 758–760.
[8] J. Zhang, Y. Wang, P. Cheng, Y.L. Yao, J. Appl. Phys. 99 (6) (2006) 064902.
[9] A.C. Tam, H.K. Park, C.P. Grigoropoulos, Appl. Surf. Sci. 127–129 (1998) 721–725.
[10] M. She, D. Kim, C.P. Grigoropoulos, J. Appl. Phys. 86 (11) (1999) 6519–6524.
[11] M. Bereznai, I. Pelsoczi, Z. Toth, K. Turz, M. Radnai, Z. Bor, A. Fazekas, Biomaterials 24 (23) (2003) 4197–4203.
[12] Ph. Delaporte, M. Gastaud, W. Marine, M. Scentis, O. Uteza, P. Thouvenot, J.L. Alcaraz, J.M. Le Samdedy, D. Blin, Appl. Surf. Sci. 208–209 (2003) 298–305.
[13] D.E. Roberts, T.S. Modise, Appl. Surf. Sci. 253 (2007) 5258–5267.
[14] X. Wang, X. Xu, J. Heat Trans. 124 (2) (2002) 265–274.
[15] T.Y. Choi, C.P. Grigoropoulos, J. Appl. Phys. 92 (9) (2002) 4918–4925.
[16] A.Q. Wu, I.H. Chowdhury, X. Xu, Phys. Rev. B 72 (8) (2005) 085128.
[17] A.J. Heltzel, A. Battula, J.R. Howell, S.C. Chen, J. Heat Trans. 129 (1) (2007) 53–59.
[18] X. Wang, X. Xu, J. Therm. Stresses 25 (5) (2002) 457–473.
[19] J.P. McDonald, J.L. Hendricks, V.R. Mistry, D.C. Martin, S.M. Yalisove, J. Appl. Phys. 102 (1) (2007) 013107.
[20] A.P. Joglekar, H.H. Liu, E. Meyhofer, G. Mourou, A.J. Hunt, PNAS 101 (16) (2004) 5856–5861.
[21] Z. Guo, S. Kumar, Appl. Opt. 40 (19) (2001) 3156–3163.
[22] K.H. Kim, Z. Guo, Numer. Heat Trans. A 46 (1) (2004) 23–46.
[23] H. Quan, Z. Guo, Opt. Exp. 12 (3) (2004) 449–457.
[24] X.L. Wang, Z. Guo, Opt. Laser Technol. 42 (2) (2010) 447–451.
[25] M.H. Niemz, Laser Tissue Interactions—Fundamentals and Applications, Springer, New York, 1996.
[26] A. Ben-Yakar, R.L. Byer, J. Appl. Phys. 96 (9) (2004) 5316–5323.
[27] F.H. Loesel, J.P. Fischer, M.H. Gotz, C. Horvath, T. Juhasz, F. Noack, N. Suhm, J.F. Bille, Appl. Phys. B 66 (1) (1998) 121–128.
[28] S. Baudach, J. Bonse, W. Kautek, Appl. Phys. A 69 (1999) S395–S398.
[29] H. Huang, Z. Guo, J. Micromech. Microeng. 19 (2009) 055007.
[30] H. Huang, Z. Guo, J. Phys. D: Appl. Phys. 42 (2009) 165204.
[31] H. Huang, Z. Guo, Laser Med. Sci. 25 (4) (2010) 517–524.
[32] S. Zoppel, H. Huber, G.A. Reider, Appl. Phys. A 89 (2007) 161–163.
[33] F. Meyer, A. Ostendorf, U. Stute, J. Phys.: Conf. Ser. 59 (2007) 408–412.